J Electr Eng Technol.2015; 10(3): 847-858
http://dx.doi.org/10.5370/JEET.2015.10.3.847

ISSN(Print) 1975-0102
ISSN(Online) 2093-7423

Coordinated Control Strategy and Optimization of Composite Energy Storage System Considering Technical and Economic Characteristics

Fengbing Li†, Kaigui Xie*, Bo Zhao, Dan Zhou**, Xuesong Zhang** and Jiangping Yang*****

Abstract – Control strategy and corresponding parameters have significant impacts on the overall technical and economic characteristics of composite energy storage systems (CESS). A better control strategy and optimized control parameters can be used to improve the economic and technical characteristics of CESS, and determine the maximum power and stored energy capacity of CESS. A novel coordinated control strategy is proposed considering the coordination of various energy storage systems in CESS. To describe the degree of coordination, a new index, i.e. state of charge coordinated response margin of supercapacitor energy storage system, is presented. Based on the proposed control strategy and index, an optimization model was formulated to minimize the total equivalent cost in a given period for two purposes. The one is to obtain optimal control parameters of an existing CESS, and the other is to obtain the integrated optimal results of control parameters, maximum power and stored energy capacity for CESS in a given period. Case studies indicate that the developed index, control strategy and optimization model can be extensively applied to optimize the economic and technical characteristics of CESS. In addition, impacts of control parameters are discussed in detail.

Keywords: Composite energy storage system, Coordinated control, Lifetime quantization, Technical and economic characteristics, Operation optimization, Integrated optimization

1. Introduction

Up to now, among all the energy storage options available in practical engineering, no single type of energy storage can fulfill all the desirable features of an ideal storage device. Energy storage devices are generally divided into energy-type storage and power-type storage. The energy-type storage, such as lithium-ion battery (LB), provides high energy capacity, low self-discharge and relatively low cost, but suffers from short cycle life which has a great relationship with its charging and discharging process. In contrast, the power-type storage, such as super-capacitor (SC), has superior cycle efficiency, a long cycle life, and capability of dealing with high power charging or discharging, but it has small energy capacity, high self-discharge rate and relatively high cost. A promising way is to exploit different types of energy storages in a composite manner, realizing the advantages of each cell while hiding their weaknesses. For example, composite energy storage system (CESS) using in practical engineering is composed of multiple different energy storages and their matching power conversion system (PCS), i.e. a plurality of energy storage systems (ESS). In order to maximize the strengths of various energy storages and to improve the overall performance, control strategy and optimization of CESS has become a research hotspot.

Control strategy, namely how to combine various ESSs of CESS, has been researched mainly in the fundamental problem, i.e. power allocation, and protection of power limit, over-charge and over-discharge. For the power allocation within CESS considering the complementary characteristics of various ESSs, the rule based method [1, 2], fuzzy control method [3], wavelet analysis method [4, 5], low-pass/high-pass filtering method [6-14] are used to exploit the advantages of various ESSs. Among these methods, the low-pass / high-pass filtering method is most commonly used, and filter time constant can be used to quantify the distribution of power command to each ESS. For protection of CESS, the output power of each ESS is individually adjusted according to the respective circumstances of over charge, over discharge and over power limit, using the direct adjustment methods [5, 8] or indirect adjustment methods such as fuzzy logic control etc. [3, 6] to protect the components of CESS. In the intensive study, namely the coordination control of various ESSs, only the literature [12] discusses overcharge and over discharge protection control scheme when the SOC of two ESSs are in the different states, and only the literature [15]

† Corresponding Author: State Key laboratory of Power Transmission Equipment & System Security, Chongqing University, and Electric Power Research Institute of State Grid Zhejiang Electric Power Corporation, China. (cqulifengbing@163.com)
* State Key laboratory of Power Transmission Equipment & System Security, Chongqing University, China. (kaiguixie@vip.163.com)
** Electric Power Research Institute of State Grid Zhejiang Electric Power Corporation, China. (zhaobozju@163.com, 179093975@qq.com, ee_zxs@163.com)
*** State Grid Sichuan Electric Power Corporation Meishan Power Supply Company, China. (yajia1987@126.com)
Received: May 20, 2014; Accepted: January 6, 2015

describes that the power-type storage remains full charge to satisfy the pulse load in microgrid, and only the literatures [1] and [6] propose that the SOC of power-type storage should be maintained at its intermediate value to maintain a certain power adjustment capability all the time.

Optimization of CESS can be divided into performance optimization for the existing CESS with fixed maximum power and fixed energy storage capacity, configuration optimization of maximum power and stored energy capacity for ESSs in CESS, and so on. With regard to performance optimization of CESS, charge allocation, charge replacement and charge migration (i.e. storage efficiency or energy loss) are optimized in [16-18] which belong to internal optimization for module units in CESS, and the effects of the lifetime influencing factor or quantization lifetime of energy-type storage are analyzed in [3, 10-12] and [19]. Prolonging the service life of energy-type storage has an important impact on the overall performance of CESS because the service life of energy type storage is usually much smaller than power-type storage. As indirect approaches to analyze the lifetime impact of energy-type storage, it shows that depth of discharge and current ripple of energy-type storage can be reduced by filter control of CESS through simulation in [11] and [12], and a method to minimize the output current fluctuation of energy-type storage in CESS is proposed in [19]. And the quantified improvement of LB lifetime effected by control strategy of CESS is directly analyzed in [3] and [10] based on the lifetime quantization model of energy-type storage. With regard to configuration optimization of CESS, the minimal configurations of maximum power and stored energy capacity of various ESSs with the requirement of renewable energy power output to be met are discussed in [5] and [20], and stored energy capacities of CESS are optimized with the optimization objective such as annualized life cycle cost in [2], one-time investment and operation costs in [21] considering lifetime quantification of all energy storage arrays. In addition, the parameters in control strategy of CESS have a certain impact on control effect, however, the filter time constant has only been considered on optimization configuration in [2], and the effect on lifetime of LB, stored energy capacity of SC-ESS has only been analyzed in [10] when the filter time constant changes.

In order to maximize the advantages and complementary nature of various energy storage, the measures i.e. overall adjustment ability optimization and limit-protect coordination control are newly increase on the basis of filtering power allocation. A control strategy including coordination between two types of ESS and overall performance optimization is proposed for CESS. The core of proposed strategy is to optimize the overall adjustment ability, accordingly the SOC coordinated response margin of SC-ESS is proposed to reflect the state coordination between two types of ESS. Meanwhile, combining lifetime quantification model and economic factor of various energy storages and their matching PCS, the technical economic optimization model of CESS is established with the objectives to meet the technical requirement of application and to minimize total loss equivalent cost of CESS. The technical economic characteristics of the existing CESS are elevated after the optimization of two main control parameters i.e. filter time constant and proposed margin index. In addition, the integrated optimization of control parameters, maximum power and stored energy capacity of ESSs have been accomplished, and the impacts of control parameters variation on required energy storage capacity, loss equivalent cost of various ESSs are analyzed in detail.

The paper is organized as follows: Section 2 illustrates the contents and process of full text. The mathematical model and lifetime quantification model of CESS are given in Section 3. The proposed coordinated control strategy of CESS and a new index are discussed in Section 4. The models of operation optimization and integrated optimization are established in Section 5. The case studies of proposed strategy, operation optimization and integrated optimization are given in Section 6. The impact of main control parameters is discussed in Section 7. Conclusion of the paper is given in Section 8.

2. Models of ESS

2.1 Mathematical model

The ESS can be charged and discharged as required, i.e. the direction and magnitude of energy exchange between the ESS and external grid is controllable. If the direction from the ESS is defined as the positive direction, then a positive value of power output indicates discharging process of the ESS, while a negative value indicates the charging process. As shown in [2, 4, 5] and [22], the power output limits and SOC of ESS considering the effect of self-discharge rate and charge-discharge efficiency are computed as (1)-(4). This is the base model of ESSs available for both LB-ESS and SC-ESS.

$$P_{c\,\mathrm{lim},ESS(\mathrm{n})} = -\min\{[\mathrm{S}_{\max,ESS} - (1-\sigma_{ESS})\mathrm{S}_{ESS(\mathrm{n-1})}] \frac{E_{r,ESS}}{\eta_{\mathrm{c},ESS}\Delta T_{com}}, \left|\mathrm{P}_{c\,\max,ESS}\right|\} \quad (1)$$

$$P_{d\,\mathrm{lim},ESS(\mathrm{n})} = \min\{[(1-\sigma_{ESS})\mathrm{S}_{ESS(\mathrm{n-1})} - \mathrm{S}_{\min,ESS}] \frac{\eta_{d,ESS}E_{r,ESS}}{\Delta T_{com}}, \mathrm{P}_{d\,\max,ESS}\} \quad (2)$$

$$\mathrm{E}_{ESS(\mathrm{n})} = \begin{cases} (1-\sigma_{ESS})E_{ESS(n-1)} - P_{out,ESS}\eta_{c,ESS}\Delta T_{com}, & (P_{out,ESS} \le 0) \\ (1-\sigma_{ESS})E_{ESS(n-1)} - \dfrac{P_{out,ESS}}{\eta_{d,ESS}}\cdot\Delta T_{com}, & (P_{out,ESS} > 0) \end{cases} \quad (3)$$

$$\mathrm{S}_{ESS(n)} = E_{ESS(n)} / E_{r,ESS} \quad (4)$$

2.2 Lifetime quantification models

As integral parts of CESS, various PCSs are usually

uninterrupted work, and their power electronic devices have a limited lifetime. Without taking into account the failure, lifetime loss coefficient of each PCS is approximately the ratio of running time and corresponding lifetime time. The coefficient is computed as (5).

$$L_{loss,PCS} = T / T_{life,PCS} \tag{5}$$

In the CESS with LB-ESS and SC-ESS, lifetime quantization models of energy storages include lifetime quantization models of both LB and SC. The charge-discharge cycles of SC are more than one million times [9, 10], which are much larger than that of LB. Therefore, an approximate calculation model is used for lifetime quantization of SC, and a detailed calculation model is used for lifetime quantization of LB. The lifetime loss coefficient of SC is approximately the ratio of run cycles and its total cycles, which is computed as (6).

$$L_{loss,SC} = N_{cycle,SC} / N_{total,SC} \tag{6}$$

The lifetime of LB is mainly considered from degradation failure that degradation of certain performance index increases gradually with time in service, and life is end when the index reaches a failure threshold. The lifetime of LB is typically defined as cycle life or calendar life corresponding with the degenerative process from the nominal energy capacity to its 80% [23-26]. Capacity degradation algorithm of LB suitable for practical applications and irregular charge-discharge application in particular is proposed in [23], as a function of the equivalent throughput cycles, the average SOC, the SOC normalized deviation and the operating temperature. The algorithm validated by experiments and actual operation has repeatedly been cited or applied directly in [18, 24-29]. According to the algorithm, the increment of LB capacity degradation in the time interval τ is computed as (7).

$$\Delta D_{LB}(m) = D_2 \cdot \exp[K_T (T_{LB} - T_{ref}) \cdot \frac{T_{a,ref}}{T_{a,LI}}] \tag{7}$$

where,

$$D_2 = D_1 \cdot \exp[4K_{SOC}(S_{avg,LB} - 0.5)] \cdot [1 - D_{LB}(m-1)]$$

$$D_1 = K_{co} N_{LB} \cdot \exp(\frac{S_{dev,LB} - 1}{K_{ex}} \cdot \frac{T_{a,ref}}{T_{a,LB}}) + \frac{0.2\tau}{\tau_{life,LB}}$$

where T_{ref}=25℃, $T_{a,ref} = T_{ref}$+273, $T_{a,LB} = T_{LB}$ +273, K_T= 0.0693, K_{co} = 3.66e-5, K_{ex} = 0.717, K_{SOC} = 0.916. The last four coefficients as given in [23] are typical values, which are used as empirical constants of a particular LB. And these coefficients can be amended in accordance with the lifetime data for different LB.

The capacity degradation of LB for M time intervals is then given by (8).

$$D_{LB}(M) = \sum_{m=1}^{M} \Delta D_{LB}(m) \tag{8}$$

The degradation D_{LB} of LB capacity as described in formula (8) changes from 0 (when LB is new) to 1 (when the capacity of LB degenerates to 0). And D_{LB}=0.2 means that the actual capacity of LB degenerates to 80% of its nominal capacity. So the lifetime loss coefficient of LB is computed as (9).

$$L_{loss,LB} = D_{LB} / 0.2 \tag{9}$$

3. Coordinated Control and New Index of CESS

3.1 Coordinated control strategy

A coordinated control strategy of CESS based on charge-discharge state of LB-ESS is proposed in order to improve the overall performance. In this strategy, power commands are allocated by the high-pass filter. Then SOC of SC-ESS is adjusted based on the charge-discharge state of LB-ESS with the purpose of overall adjustment ability optimization. And the protection coordination between two ESSs is implemented for over-charge protection, over-discharge protection and maximum power limit. The control block diagram and control flow chart of the strategy are given as Fig. 1.

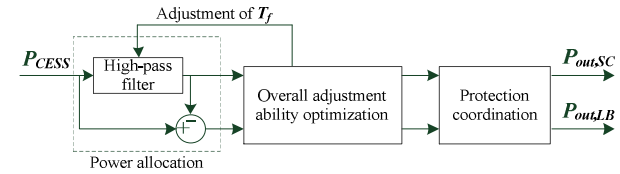

(a) Control block diagram

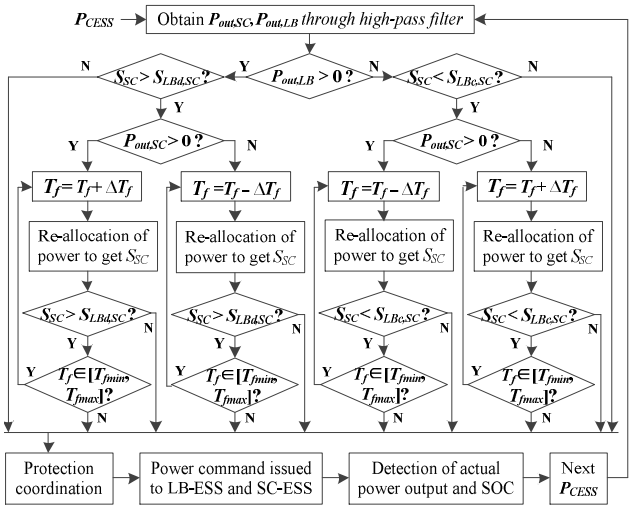

(b) Control flow chart

Fig. 1. Coordinated control strategy of CESS

When allocating power in CESS, the high-frequency fluctuation power of P_{CESS} is separated by a high-pass filter and absorbed by SC-ESS, and the remaining power is absorbed by LB-ESS. The power allocations are computed as follows.

$$P_{out,SC}(s) = P_{CESS}(s) \cdot [sT_f / (1+sT_f)] \quad (10)$$

$$P_{\text{out},LB}(s) = P_{CESS}(s) - P_{out,SC}(s) = P_{CESS}(s) / (1+sT_f) \quad (11)$$

When optimizing the overall adjustment ability, the usage of state coordinating between two ESSs is demanded. The stored energy of SC-ESS is maintained at a lower level when LB-ESS is discharging, and maintained at a higher level when LB-ESS is charging. In order to make SOC of SC-ESS to achieve the different control objectives set by the charge-discharge states of LB-ESS as far as possible, the time constant T_f should be repeatedly adjusted within the permissible range [T_{fmin}, T_{fmax}] in steps of ΔT_f, where $T_{fmax} = T_{f0} + T_{flim}$, and $T_{fmin} = \max(0, T_{f0} - T_{flim})$.

When protection coordination is in progress, there is a need for coordination between two ESSs of CESS. The output power of ESSs should be adjusted due to over-charge protection, over-discharge protection and maximum power limit, at the same time the adjusted part of output power could be undertook by the other ESS within its allowable range.

3.2 Coordinated response margin of SC-ESS

Fig. 2 illustrates the principle of overall adjustment ability optimization as the core part of the proposed strategy, where SOC of SC-ESS is dynamically adjusted according to charge-discharge status of LB-ESS. It shows that charging margin is reserved in SC-ESS when LB-ESS is discharging, and discharging margin is reserved in SC-ESS when LB-ESS is charging. Then there will be an enhanced response capability for instantaneous power changes, an optimization of charge and discharge process for LB-ESS, and an improvement of overall performance for CESS. Hence, a new index named as SOC coordinated response margin of SC-ESS is proposed and denoted by $\Delta S_{co,SC}$, which is numerically equal to ($S_{max,SC} - S_{LBd,SC}$) or ($S_{LBc,SC} - S_{min,SC}$). And there is a relation described as $S_{max,SC} - S_{LBd,SC} = S_{LBc,SC} - S_{min,SC}$ because the charging margin is equal to the discharge margin due to their interlinked principle.

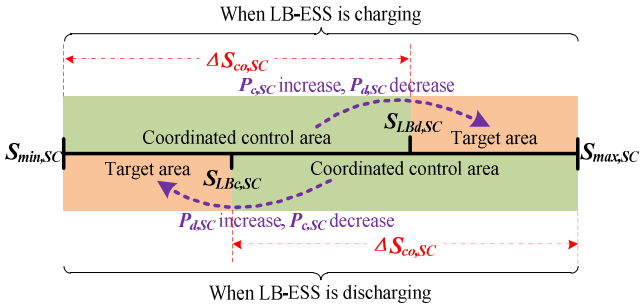

Fig. 2. Coordinated control diagram of overall adjustment ability optimization

4. Optimization Model of CESS

4.1 Objective function

Technical characteristic of CESS can be considered consistent when PCESS is met by output powers of the internal ESSs all the time. Economic characteristic of CESS can be reflected by total acquisition cost or total loss equivalent cost, where the former represents only disposable investment cost and the latter considering as a comprehensive evaluation from the aspect of life cycle represents total lifetime loss quantization of CESS in a specific time. Meanwhile, the objective to minimize total loss equivalent cost within a certain time is used for operation optimization and integrated optimization of CESS based on consideration of comparability. In summary, a mathematical model of CESS technical economic optimization is proposed as follow.

$$\min(C_{equ,CESS}) = \min(C_{equ,\text{LB}} + C_{equ,SC} + C_{pen}) \quad (12)$$

where,

$$C_{equ,LB} = L_{loss,LB} \cdot (C_{unit,LB} E_{r,LB}) + L_{loss,PCS} C_{PCS,LB}$$

$$C_{equ,SC} = L_{loss,SC} \cdot (C_{unit,SC} E_{r,SC}) + L_{loss,PCS} C_{PCS,SC}$$

$$C_{pen} = \begin{cases} 0, & (P_{out,LB} + P_{out,SC} = P_{CESS}) \\ F, & else \end{cases}$$

As shown in (12), the maximum power of an ESS is commonly limited by PCS, while its stored energy capacity is commonly affected by the number of series-parallel modules in energy storage. PCS used in the actual project is usually complete equipment, and is different required for different ESSs, e.g. single-stage PCS and dual-stage PCS used in LB-ESS and SC-ESS respectively.

4.2 Operation optimization

Operation optimization is to optimize the main parameters of the proposed control strategy in an existing CESS wherein all ESSs have an assured maximum power and stored energy capacity, using optimization model shown as (12). The minimum of total loss equivalent cost within a certain time can be obtained for CESS while satisfying the same power requirement. The parameters to be optimized are the proposed strategy's main control parameters T_f and $\Delta S_{co,SC}$. Constraint conditions of operation optimization are provided as follows.

2) SOC operating ranges of ESSs

$$S_{\min,LB} \le S_{LB} \le S_{\max,LB} \quad (13)$$

$$S_{\min,SC} \le S_{SC} \le S_{\max,SC} \quad (14)$$

2) Output power limits of ESSs

$$P_{c\lim,LB} \le P_{out,LB} \le P_{d\lim,LB} \quad (15)$$

$$P_{c\lim,SC} \le P_{out,SC} \le P_{d\lim,SC} \quad (16)$$

3) SOC coordinated response margin range of SC-ESS

$$0 \le \Delta S_{co,SC} \le (S_{\max,SC} - S_{\min,SC}) \quad (17)$$

4.3 Integrated optimization

Integrated optimization is to optimize the main parameters of the proposed control strategy, together with the required maximum power and required energy capacity of all ESSs in CESS, using optimization model shown as (12). The minimum of total loss equivalent cost within a certain time can be obtained for CESS while satisfying the same power requirement. The parameters to be optimized are the proposed strategy's main control parameters T_f, $\Delta S_{co,SC}$, the ESSs' required maximum power $P_{r,LB}$, $P_{r,SC}$ and required energy storage capacity $E_{r,LB}$, $E_{r,SC}$. In addition to (13) ~ (17), constraint conditions of integrated optimization include maximum power range of ESSs shown as follows.

$$P_{r,LB} \in \{50,100,200,250,300,400,500,...\} \quad (18)$$

$$P_{r,SC} \in \{50,100,200,250,300,400,500,...\} \quad (19)$$

In the engineering applications, PCS of ESS generally uses standard equipment package, which make the maximum power of ESSs to be one of the few optional specification values, such as 50kW, 100kW, 200kW, 250kW, 300kW, 400kW, 500kW, etc. The stored energy capacity of ESS is mainly affected by the number of series-parallel modules in energy storage, and can be considered as approximate continuous change when the module number is increased or decreased.

Meanwhile, the maximum power and stored energy capacity of ESSs are considered in the integrated optimization, so the acquisition cost of CESS as an assistant index of technical economic comparison for integrated optimization will be affected directly [30]. The acquisition cost of CESS comprising of LB-ESS and SC-ESS is computed as (20).

$$C_{acq,HESS} = C_{acq,LB} + C_{acq,SC} \quad (20)$$

where,

$$C_{acq,LB} = C_{unit,LB} E_{r,LB} + C_{PCS,LB}$$

$$C_{acq,SC} = C_{unit,SC} E_{r,SC} + C_{PCS,SC}$$

5. Case Studies

The parameters in the simulation are set as ΔT_f=1, T_{flim}=10, F=10,000$. The output power command of CESS, which is the operation curve of ESS taking as the system main power supply in an island independent microgrid, is shown in Fig. 3. The main parameters of LB-ESS and SC-ESS are provided in Table 1, where the matching PCSs typically have a lifetime of 10 years, and their acquisition costs are shown in Table 2.

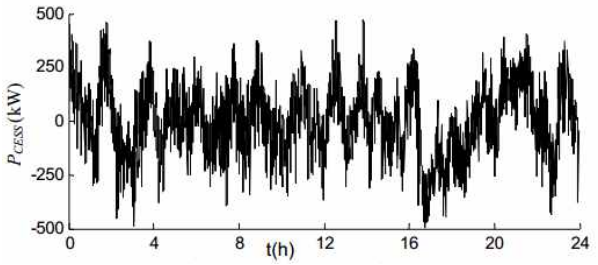

Fig. 3. The power command of CESS

Table 1. Main parameter settings of two ESSs

Parameter type	LB-ESS	SC-ESS
Operating range of SOC	0.25~0.95	0.2~0.9
SOC threshold of over-charge protection	0.9	0.85
SOC threshold of over-discharge protection	0.3	0.25
Initial value of SOC	0.8	0.8
Charge and discharge efficiency	90%	95%
Self-discharge rate (%·s^{-1})	0	0.00017
Maximum power (kW)	500	500
Stored energy capacity (kWh)	1000	10
Unit capacity cost ($·kWh^{-1})	655.7	157,377.0

Table 2. Acquisition cost of the matching PCS for two ESSs

$P_{r,PCS}$ (kW)	50	100	200	250	300	400	500
$C_{PCS,LB}$ (10^4·$)	1.00	1.97	3.77	4.61	5.41	6.89	8.20
$C_{PCS,SC}$ (10^4·$)	1.21	2.36	4.52	5.54	6.49	8.26	9.84

5.1 Technical economic comparison between base strategy and proposed strategy

Taking into account overall adjustment ability optimization, which is the core of proposed coordinated control strategy and the main improvement different from other CESS control strategies [1-14], a contrast strategy without this optimization is set and named base strategy. The filter time constant T_f is set as 30 in the base strategy and proposed strategy, and the margin indicator $\Delta S_{co,SC}$ is set as 0.35 in the proposed strategy, i.e. SOC control objective of SC-ESS is set as the average value of its maximum and minimum. When the power command shown in Fig. 3 is met in two strategies respectively, the power output curve and SOC curve of ESSs are given in Fig. 4.

As seen in Fig. 4, the SOC of SC-ESS is closed to its limit for a long time in the absence of an orderly control,

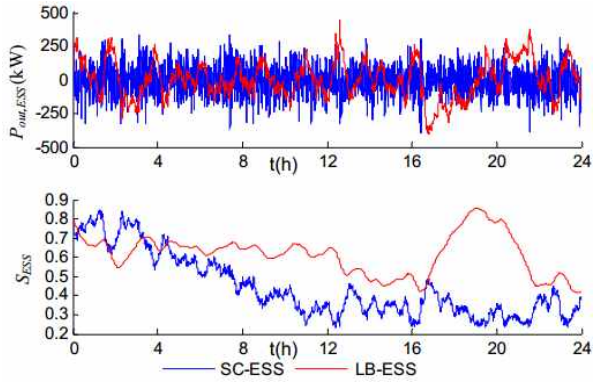

(a) The results under the base strategy

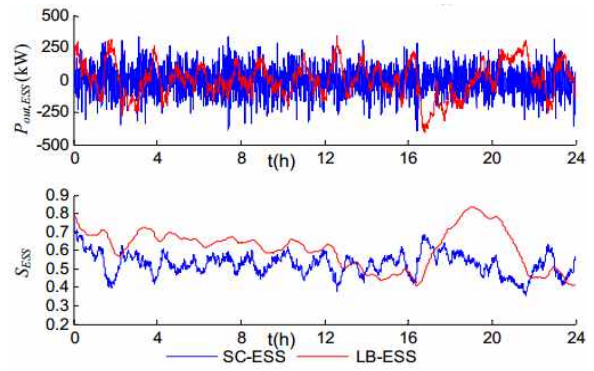

(b) The results under the proposed strategy

Fig. 4. Output power and SOC of two ESSs using two strategies

Table 3. Lifetime loss and equivalent cost of ESSs using two strategies

	$L_{loss,LB}$ (10^{-3})	$L_{loss,SC}$ (10^{-5})	$C_{equ,LB}$ ($)	$C_{equ,SC}$ ($)	$C_{equ,CESS}$ ($)
Base Strategy	1.0374	1.8655	702.72	56.31	759.03
Proposed Strategy	0.9895	1.8680	671.30	56.35	727.65

resulting in a significant decrease in their ability to participate in the system power regulation. By contrast, state adjustment of SC-ESS using the proposed strategy keeps its SOC in a reasonable range all the time through coordination between two ESSs, and thereby always maintaining a certain ability to regulate power.

The lifetime loss and equivalent cost of ESSs using the base strategy and the proposed strategy are given in Table 3. Compared with base strategy, the lifetime loss of LB arrays within the simulation time using proposed strategy is decreased significantly by 4.62%, and the decrease in equivalent cost of LB-ESS is 4.47%. At the same time, there is a slight increase in the lifetime loss of SC array as well as the equivalent cost of SC-ESS. And the total equivalent cost of CESS lifetime loss is significantly reduced by 4.13%.

In summary, the technical economic characteristics of CESS when using the proposed strategy is significantly better than using the base strategy through the coordination and cooperation between two ESSs.

5.2 Improvement in technical economic characteristics after operation optimization

The results of operation optimization based on the proposed strategy are provided in Table 4, where the results are from the solution of optimization model shown in (12) using particle swarm optimization algorithm.

Compared with the non-optimization control parameters of the proposed strategy, the total equivalent cost of CESS lifetime loss as shown in Tables 3 and Table 4 is significantly decreased by 3.59% after optimizing. Specifically, the lifetime loss of LB-ESS and SC-ESS are both significantly decreased by 3.42 % and 13.47 % respectively, and the equivalent cost of LB-ESS and SC-ESS are both significantly decreased by 3.30% and 7.05% respectively.

Consequently, operation optimization of the existing CESS can significantly enhance its overall technical economic characteristics by optimizing filter time constant and margin index.

Table 4. Operation optimization result of CESS using proposed strategy

T_f	$\Delta S_{co,SC}$	$L_{loss,LB}$ (10^{-3})	$L_{loss,SC}$ (10^{-5})	$C_{equ,LB}$ ($)	$C_{equ,SC}$ ($)	$C_{equ,CESS}$ ($)
15	0.52	0.9557	1.6163	649.13	52.38	701.51

5.3 Improvement of technical economic characteristics after integrated optimization

In the integrated optimization of CESS, the parameters of ESSs are shown as Table 1 and Table 2 except the maximum power and stored energy capacity. Then the optimization model given in formula (12) is solved using particle swarm optimization algorithm based on the proposed strategy, and the optimal result of integrated optimization is provided in Table 5. Moreover, the results of operation optimization and integrated optimization are put together to facilitate comparative analysis. The gray parts of Table 5 show that the maximum power, stored energy capacity and acquisition cost of two ESSs are all fixed values in operation optimization.

In Table 5, it shows that,

1) The parameters to be optimized of operation optimization are T_f and $\Delta S_{co,SC}$, the proposed strategy's main control parameters. And their optimal values are 15 and 0.52 respectively. At the same time, the parameters to be optimized of integrated optimization are the required maximum power $P_{r,LB}$, $P_{r,SC}$, the required energy storage capacity $E_{r,LB}$, $E_{r,SC}$, the proposed strategy's main control parameters T_f, $\Delta S_{co,SC}$. And their optimal values are 500, 300, 761.80, 3.12, 23 and 0.53 respectively.
2) Comparing with the lifetime loss and homologous

Table 5. Operation optimization result and integrated optimization result of CESS using proposed strategy

	Parameters						Lifetime loss and equivalent cost					Acquisition cost		
	$P_{r,LB}$ (kW)	$P_{r,SC}$ (kW)	$E_{r,LB}$ (kWh)	$E_{r,SC}$ (kWh)	T_f	$\Delta S_{co,SC}$	$L_{loss,LB}$ (10^{-3})	$L_{loss,SC}$ (10^{-5})	$C_{equ,LB}$ ($)	$C_{equ,SC}$ ($)	$C_{equ,CESS}$ ($)	$C_{acq,LB}$ (10^4·$)	$C_{acq,SC}$ (10^4·$)	$C_{acq,CESS}$ (10^4·$)
Operation optimization	500	500	1000	10	15	0.52	0.9557	1.6163	649.13	52.38	701.51	73.77	167.21	240.98
Integrated optimization	500	300	761.80	3.12	23	0.53	0.8515	5.6808	447.83	45.64	493.48	58.15	55.54	113.69

equivalent cost of ESSs after operation optimization, there are many benefits for the integrated optimization of CESS. For example, the lifetime loss of LB is significantly reduced by 10.90%, the equivalent cost of LB-ESS is substantially decreased by 31.01%, the equivalent cost is significantly decreased by 12.87% while lifetime loss of SC is amplified more than three times, and that total lifetime loss equivalent cost of CESS is substantially decreased by 29.65%.

3) From the further analysis combined with acquisition cost of ESSs, through the integrated optimization of CESS, there is not only a sharp fall in the total lifetime loss equivalent cost of CESS because of the substantial decrease in maximum power and stored energy capacity of ESSs, but also a decrease of 1.2729 million dollars in the $C_{equ,CESS}$, i.e. a reduction up to 52.82%.

The previous analysis has shown that, comparing with the optimal result of operation optimization for the existing CESS, the integrated optimization of CESS can not only significantly reduce the total lifetime loss equivalent cost of CESS in a certain time, but also decrease its acquisition cost by more than half. So the technical economic characteristics has increased substantially both in initial investment cost and life cycle cost after the integrated optimization.

6. Impact Analysis of Control Parameters

Setting T_f as a fixed value, an optimal result of CESS integrated optimization can be computed by optimization model shown in (12). When T_f is set as different fixed values, the different optimal results can be obtained by re-optimization, and the variation trends of optimal results with change of T_f will be obtained. The variation trends of optimal results with the set value of $\Delta S_{co,SC}$ change can get in the same way. The variation range of T_f is set as {11, 12,…, 30} according to the results of integrated optimization in Table V, and the variation range of $\Delta S_{co,SC}$ is set as {0.05, 0.10, …, 0.65} according to its range constraint. In the light of the analysis of the optimal result, the influence of two control parameters presents certain regularity.

6.1 Impact analysis of T_f

As shown in Fig. 5, the minimal $C_{equ,CESS}$ decreases firstly and then increases as the constant T_f is increased.

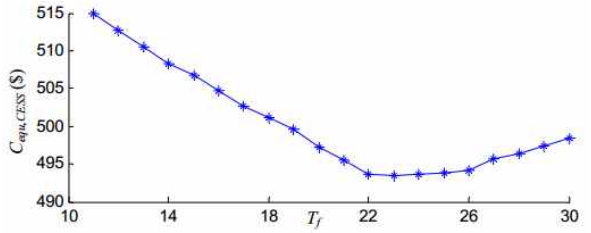

Fig. 5. Curve of optimal $C_{equ,CESS}$ with changes in T_f

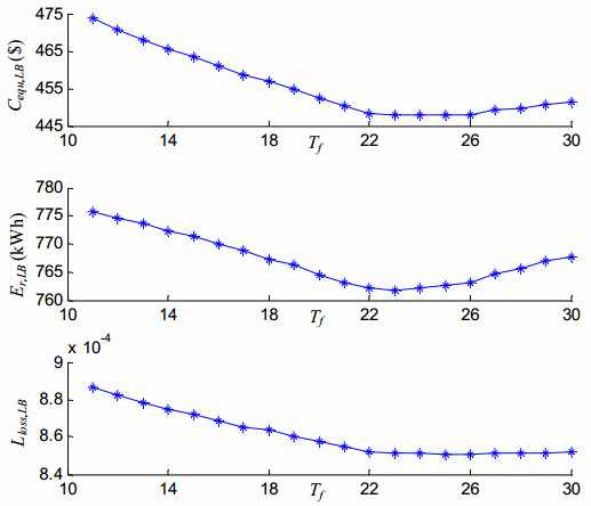

Fig. 6. Curves of relevant data for LB-ESS with changes in T_f

For LB-ESS in CESS, the minimum of $C_{equ,LB}$ is decreased firstly and then increased slightly with increase of T_f as illustrated in Fig. 6. As Tf increaseing, the lifetime loss of LB is reduced gradually, and the required energy capacity is reduced firstly and then increased slightly. The slight increase of required energy capacity is normal, because in order to get a better smoothness the power output of LB-ESS needs to increase when T_f is larger than certain threshold.

For SC-ESS in CESS, the minimum of $C_{equ,LB}$ is increased constantly as illustrated in Fig. 7. As T_f increasing, the required energy capacity of SC-ESS is increased constantly, and the lifetime loss of SC is reduced gradually.

In conclusion, the detailed effects of different control parameter on CESS and ESSs inside are got. For example, when T_f increases, the frequency domain range of high-frequency fluctuation of P_{CESS} born by SC-ESS becomes

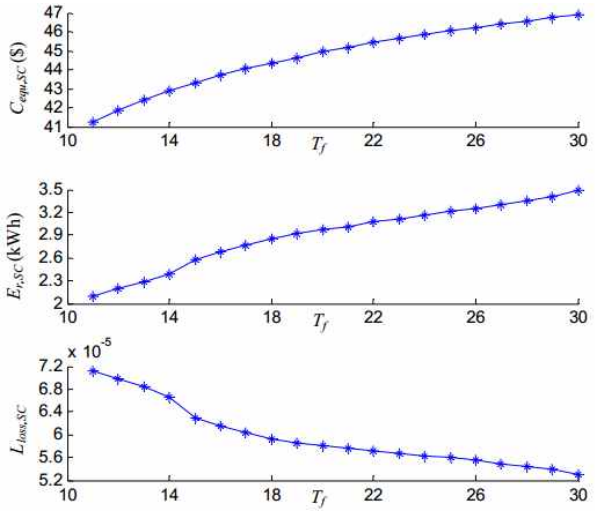

Fig. 7. Curves of relevant data for SC-ESS with changes in T_f

larger and the power output of SC-ESS is increased, and this will lead to a continuous increase in the required energy storage capacity of SC-ESS and a gradual rise in the lifetime loss equivalent cost of SC-ESS. At the same time, the output power of LB-ESS will become smoother, and the lifetime loss and corresponding equivalent cost will decrease gradually. The change tendency of lifetime loss equivalent cost in two ESSs is just opposite, but the total cost $C_{equ,CESS}$ is decreased firstly and then increased, and the turning point is the optimal point.

6.2 Impact analysis of $\Delta S_{co,SC}$

When the parameters except T_f as fixed value is optimizing, the optimal $\Delta S_{co,SC}$ corresponding to different T_f is within the compass of 0.50~0.53 as illustrated in Fig. 8, while the value range of $\Delta S_{co,SC}$ is 0~0.7.

The results of integrated optimization with different values of $\Delta S_{co,SC}$ in its permissible range Figs. 9 and Fig. 10. As $\Delta S_{co,SC}$ increasing, the optimal values of T_f increase firstly and then decrease. Meanwhile, for LB-ESS, $E_{r,LB}$ and $C_{equ,LB}$ both decrease firstly and then increase, and for SC-ESS, $E_{r,SC}$ decrease firstly and then increase while $C_{equ,LB}$ increase firstly and then decrease, and for CESS, the total cost $C_{equ,CESS}$ is decreased firstly and then increased, and the turning point is the optimal point.

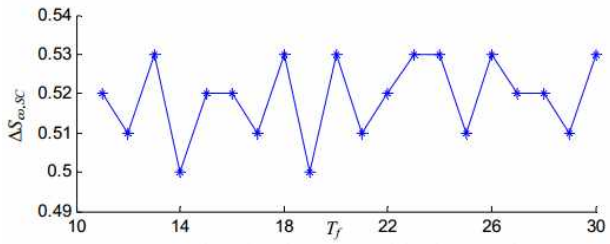

Fig. 8. Curve of optimal $\Delta S_{co,SC}$ with changes in T_f

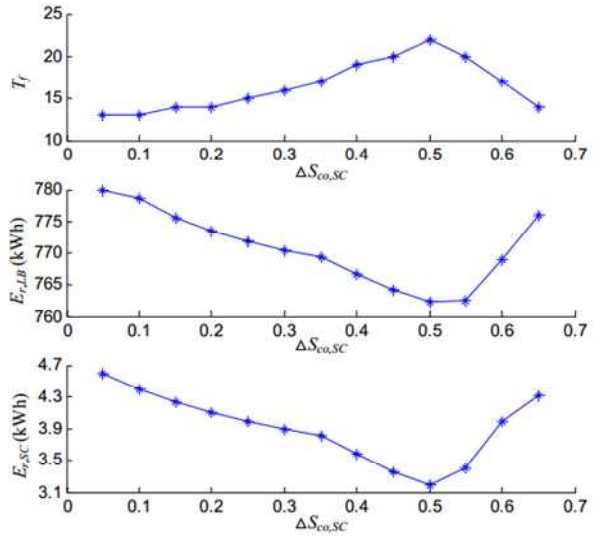

Fig. 9. Optimal results of parameters with changes in $\Delta S_{co,SC}$

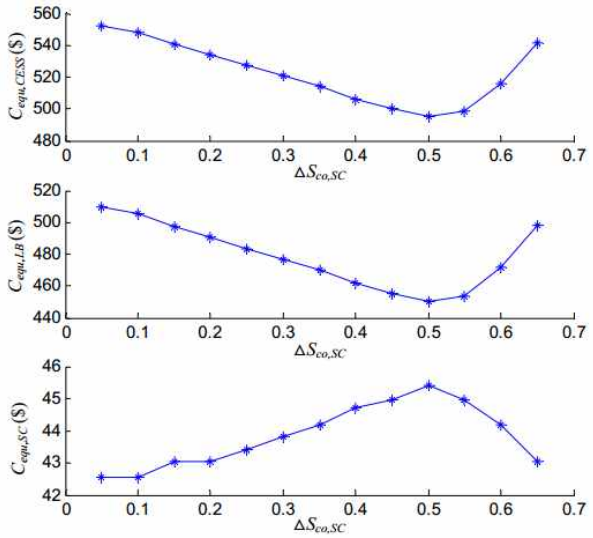

Fig. 10. Optimal results with changes in $\Delta S_{co,SC}$

7. Conclusion

A novel entirety control strategy of CESS is presented in this paper based on the power allocation method. Compared with no regard to the overall adjustment ability optimization, the proposed strategy can always maintain a certain ability in SC-ESS to regulate power output, and obviously improve the overall technical economic characteristics of CESS.

The proposed overall adjustment ability optimization which dynamically adjusts SOC of SC-ESS according to the charge-discharge state of LB-ESS can quantify coordination between two ESSs by the margin index. The optimization case study of two main control parameters shows that the technical economic characteristics of the existing CESS have improved significantly by operation

optimization.

The impact of control parameters should be considered in integrated optimization of CESS where maximum power and stored energy capacity of various ESSs is optimized. Case study of integrated optimization shows that the total loss equivalent cost, required maximum power, required energy storage capacity and one-time investment are all substantially decreased. Furthermore, the impact analysis of margin index and filter time constant show that only when the filter time constant and margin index are all moderate size, the technical economic characteristics of CESS can be optimal.

The characteristics of ESS used in practical application have been fully considered in this paper, such as the impact of self-discharge rate and charge-discharge efficiency in mathematical model, lifetime quantification of all energy storages and their matching PCS, the characteristics of PCS which is usually complete equipment and different for different ESS, and so on. Therefore the researches here are more reasonable and have more reference value. The coordinated control strategy and technical economic optimization method will be used in practical engineering as the follow work, and a further research and discussion will be done soon.

Acknowledgements

This work is supported by National High Technology Research and Development Program of China (863 Program) (No.2011AA05A107).

Nomenclature

LB	Lithium-ion battery
SC	Supercapacitor
CESS	Composite energy storage system
PCS	Power conversion system
ESS	Energy storage system
LB-ESS	Lithium-ion battery energy storage system
SC-ESS	Supercapacitor energy storage system
SOC	State of charge
T	Running time of system
ΔT_{com}	Time step of computation
$P_{out,ESS}$	Output power of ESS
$P_{cmax,ESS}$	Maximum charging power of ESS
$P_{dmax,ESS}$	Maximum discharging power of ESS
$P_{clim,ESS(n)}$	Charging power limit of ESS in the current period
$P_{dlim,ESS(n)}$	Discharging power limit of ESS in the current period
$P_{r,ESS}$	Rated power of ESS
$E_{r,ESS}$	Rated capacity of ESS
$S_{max,ESS}$	Maximum SOC of ESS
$S_{min,ESS}$	Minimum SOC of ESS
$E_{ESS(n)}$	Stored electric energy of ESS at the current moment
$E_{ESS(n-1)}$	Stored electric energy of ESS at the previous moment
$S_{ESS(n)}$	SOC of ESS at the current moment
$S_{ESS(n-1)}$	SOC of ESS at the previous moment
σ_{ESS}	Self-discharge rate of ESS
$\eta_{c,ESS}$	Charging efficiency of ESS
$\eta_{d,ESS}$	Discharging efficiency of ESS
$T_{life,PCS}$	Lifetime of PCS
$L_{loss,PCS}$	Lifetime loss coefficient of PCS
$N_{cycle,SC}$	Charge and discharge cycles of SC
$N_{total,SC}$	Total charge and discharge cycles of SC
$L_{loss,SC}$	Lifetime loss coefficient of SC
τ	Certain time interval
ΔD_{LB}	Degenerate increment of LB capacity
D_1	Intermediate variable of ΔD_{LB}
D_2	Intermediate variable of ΔD_{LB}
$S_{avg,LB}$	SOC average value of LB
$S_{dev,LB}$	SOC normalized deviation of LB
N_{LB}	Equivalent throughput cycle of LB
T_{ref}	Reference temperature in degrees centigrade
T_{LB}	Operation temperature of LB in degrees centigrade
$T_{a,ref}$	Absolute temperature of T_{ref}
$T_{a,LB}$	Absolute temperature of T_{LB}
$\tau_{life,LB}$	Calendar lifetime estimate of LB end of 80% initial capacity
K_T, K_{co}, K_{ex}, K_{SOC}	Empirical constant of specific LB
D_{LB}	Degradation of LB capacity
$\Delta D_{LB}(m)$	Degenerate increment of LB capacity in time interval m
$D_{LB}(m-1)$	Degradation of LB capacity for m-1 time intervals
$D_{LB}(M)$	Degradation of LB capacity for M time intervals
$L_{loss,LB}$	Lifetime loss coefficient of LB
P_{CESS}	Power command of CESS
$P_{out,LB}$	Output power of LB-ESS
$P_{out,SC}$	Output power of SC-ESS
T_f	Filter time constant
T_{f0}	Initial value of Tf in power allocation
ΔT_f	Adjustment step of T_f
T_{flim}	Adjustment width of T_f
T_{fmin}	Minimum of T_f Adjustment
T_{fmax}	Maximum of T_f Adjustment
S_{SC}	SOC of SC-ESS
$S_{min,SC}$	Minimum SOC of SC-ESS
$S_{max,SC}$	Maximum SOC of SC-ESS
$S_{LBd,SC}$	SOC control objective of SC-ESS when LB-ESS discharges
$S_{LBc,SC}$	SOC control objective of SC-ESS when LB-ESS charges
$\Delta S_{co,SC}$	SOC coordinated response margin of SC-ESS
$C_{equ,CESS}$	Loss equivalent cost of CESS
$C_{equ,LB}$	Loss equivalent cost of LB-ESS

$C_{equ,SC}$ Loss equivalent cost of SC-ESS
$C_{unit,LB}$ Unit energy capacity cost of LB-ESS
$C_{PCS,LB}$ Acquisition cost of the matching PCS for LB-ESS
$C_{unit,SC}$ Unit energy capacity cost of SC-ESS
$C_{PCS,SC}$ Acquisition cost of the matching PCS for SC-ESS
C_{pen} Penalty cost without meeting the system power balance
F Fixed value much larger than $C_{equ,CESS}$
S_{LB} SOC of LB-ESS
$S_{min,LB}$ Minimum SOC of LB-ESS
$S_{max,LB}$ Maximum SOC of LB-ESS
$P_{clim,LB}$ Charging power limit of LB-ESS
$P_{dlim,LB}$ Discharging power limit of LB-ESS
$P_{clim,SC}$ Charging power limit of SC-ESS
$P_{dlim,SC}$ Discharging power limit of SC-ESS
$P_{r,LB}$ Required power rating of LB-ESS
$E_{r,LB}$ Required energy capacity of LB-ESS
$P_{r,SC}$ Required power rating of SC-ESS
$E_{r,SC}$ Required energy capacity of SC-ESS
$C_{acq,CESS}$ Acquisition cost of CESS
$C_{acq,LB}$ Acquisition cost of LB-ESS
$C_{acq,SC}$ Acquisition cost of SC-ESS

References

[1] Z. Ding, C. Yang, Z. Zhang, C. Wang, and S. Xie, "A novel soft-switching multiport bidirectional DC-DC converter for hybrid energy storage system," *IEEE Trans. Power Electron.*, vol. 29, no. 4, pp. 1595-1609, Apr. 2014.

[2] K. W. Wee, S. S. Choi, and D. M. Vilathgamuwa, "Design of a least-cost battery-supercapacitor energy storage system for realizing dispatchable wind power," *IEEE Tans. Sustain. Energy*, vol. 4, no. 3, pp. 786-796, Jul. 2013.

[3] X. Feng, H. B. Gooi, and S. X. Chen, "Hybrid energy storage with multimode fuzzy power allocator for PV systems," *IEEE Tans. Sustain. Energy*, vol. 5, no. 2, pp. 389-397, Apr. 2014.

[4] C. Sen, Y. Usama, T. Carciumaru, X. Lu, and N. C. Kar, "Design of a novel wavelet based transient detection unit for in-vehicle fault determination and hybrid energy storage utilization," *IEEE Tans. Smart Grid*, vol. 3, no. 1, pp. 422-433, Mar. 2012.

[5] Q. Jiang, and H. Hong, "Wavelet-based capacity configuration and coordinated control of hybrid energy storage system for smoothing out wind power fluctuations," *IEEE Trans. Power Syst.*, vol. 28, no. 2, pp. 1363-1372, May 2013.

[6] T. Ise, M. Kita, and A. Taguchi, "A hybrid energy storage with a SMES and secondary battery," *IEEE Trans. Appl. Supercond.*, vol. 15, no. 2, pp. 1915-1918, Jun. 2005.

[7] S. Lemofouet, and A. Rufer, "A hybrid energy storage system based on compressed air and supercapacitors with maximum efficiency point tracking (MEPT)," *IEEE Trans. Ind. Electron.*, vol. 53, no. 4, pp. 1105-1115, Aug. 2006.

[8] H. Zhou, T. Bhattacharya, D. Tran, T. S. T. Siew, and A. M. Khambadkone, "Composite energy storage system involving battery and ultracapacitor with dynamic energy management in microgrid applications," *IEEE Trans. Power Electron.*, vol. 26, no. 3, pp. 923-930, Mar. 2011.

[9] O. C. Onar, and A. Khaligh, "A novel integrated magnetic structure based DC/DC converter for hybrid battery / ultracapacitor energy storage systems," *IEEE Tans. Smart Grid*, vol. 3, no. 1, pp. 296-307, Mar. 2012.

[10] A. M. Gee, F. V. P. Robinson, and R. W. Dunn, "Analysis of battery lifetime extension in a small-scale wind-energy system using supercapacitors," *IEEE Trans. Energy Convers.*, vol. 28, no. 1, pp. 24-33, Mar. 2013.

[11] N. Mendis, K. M. Muttaqi, and S. Pereta, "Management of low and high frequency power components in demand-generation fluctuations of a DFIG based wind dominated RAPS system using hybrid energy storage," *IEEE Trans. Ind. Appl.*, vol. 50, no. 3, pp. 2258-2268, May 2014.

[12] J. W. Shim, Y. Cho, S. Kim, S. W. Min and K. Hur, "Synergistic control of SMES and battery energy storage for enabling dispatchability of renewable energy sources," *IEEE Trans. Appl. Supercond.*, vol. 15, no. 2, pp. 1915- 1918, Jun. 2005.

[13] N. Mendis, K. M. Muttaqi, and S. Perera, "Management of battery-supercapacitor hybrid energy storage and syschronous condenser for isolated operation of PMSG based variable-speed wind turbine generating systems," *IEEE Tans. Smart Grid*, vol. 5, no. 2, pp. 944-953, Mar. 2014.

[14] W. Li, G. Joos, and J. Belanger, "Real-time simulation of a wind turbine generator coupled with a battery supercapacitor energy storage system," *IEEE Trans. Ind. Electron.*, vol. 57, no. 4, pp. 1137-1145, Apr. 2010.

[15] A. Mohamed, V. Salehi, and O. Mohammed, "Real-time energy management algorithm for mitigation of pulse loads in hybrid microgrids," *IEEE Tran. Smart Grid*, vol. 3, no. 4, pp. 1911-1922, Dec. 2012.

[16] Q. Xie, Y. Kim, Y. Wang, J. Kim, N. Chang, and M. Pedram, "Principles and efficient implementation of charge replacement in hybrid electrical energy storage systems," *IEEE Trans. Power Electron.*, vol. 29, no. 11, pp. 6110-6123, Nov. 2014.

[17] Q. Xie, Y. Kim, Y. Wang, J. Kim, N. Chang, and M. Pedram, "Single-source, single-destination charge migration in hybrid electrical energy storage systems," *IEEE Trans. Very Large Scale Integr. (VLSI) Syst.*, vol. 22, no. 12, pp. 2752-2765, Dec. 2014.

[18] Q. Xie, Y. Wang, Y. Kim, M. Pedram, and N. Chang,

"Charge allocation in hybrid electrical energy storage systems," *IEEE Trans. Comput. Aided Des. Integr. Circuits Syst.*, vol. 32, no. 7, pp. 1003-1016, Jul. 2013.
[19] M. Choi, S. Kim, and S. Seo, "Energy management optimization in a battery/supercapacitor hybrid energy storage system," *IEEE Tran. Smart Grid*, vol. 3, no. 1, pp. 463-472, Mar. 2012.
[20] S. W. Min, S. J. Kim, and D. Hur, "Optimized Installation and operations of battery energy storage system and electric double layer capacitor modules for renewable energy based intermittent generation", *J. Electr. Eng. Technol.*, vol. 8, no. 2, pp. 238-243, Aug. 2013.
[21] T. Zhou, and W. Sun, "Optimization of battery-supercapacitor hybrid energy storage station in wind/solar generation system," *IEEE Tans. Sustain. Energy*, vol. 5, no. 2, pp. 408-415, Apr. 2014.
[22] S. J. Kazempour, M. P. Moghaddam, M. R. Haghifam, and G. R. Yousefi, "Electric energy storage systems in a market-based economy: comparison of emerging and traditional technologies," *Renewable energy*, vol. 34, no. 12, pp. 2630-2639, Jun. 2009.
[23] A. Millner, "Modeling lithium ion battery degradation in electric vehicles," in *Proc. IEEE Conf. Innov. Technol. Efficient Rel. Elect. Supply*, Sep. 2010, pp. 349-356.
[24] Q. Xie, X. Lin, Y. Wang, M. Pedram, D. Shin, and N. Chang, "State of health aware charge management in hybrid electrical energy storage systems," in *Proc. Des., Autom. Test Eur. Conf. Exhib.*, Mar. 2012, pp. 1060-1065.
[25] Q. Xie, S. Yue, M. Pedram, D. Shin, and N. Chang, "Adaptive thermal management for portable system batteries by forced convection cooling," in *Proc Des., Autom. Test Eur. Conf. Exhib.*, Mar. 2013, pp. 1225-1228.
[26] L.Lam, and P.Bauer, "Practical capacity fading model for Li-ion battery cells in electric vehicles," *IEEE Trans. Power Electron.*, vol. 28, no. 12, pp. 5910-5918, Dec. 2013.
[27] C. R. Vergara, "Parametric interface for battery energy storage systems providing ancillary services," in *Proc. IEEE 3rd PES Innov. Smart Grid Technol. Eur.*, 2012, pp. 1-7.
[28] J. Traube, F. Lu, D. Maksimovic, J. Mossoba, M. Kromer, P. Faill, S. Katz, B. Borowy, S. Nichols, and L. Casey, "Mitigation of solar irradiance intermittency in photovoltaic power systems with integrated electric-vehicle charging functionality," *IEEE Trans. Power Electron.*, vol. 28, no. 6, pp. 3058-3067, Jun. 2013.
[29] P. Grahn, J. Munkhammar, J. Widen, K. Alvehag, and L. Soder, "PHEV home-charging model based on residential activity patterns," *IEEE Trans. Power Syst.*, vol. 28, no. 3, pp. 2507-2515, Aug. 2013.
[30] P. Poonpun, and W. T. Jewell, "Analysis of the cost per kilowatt hour to store electricity," *IEEE Trans. Energy Convers.*, vol. 23, no. 2, pp. 529-534, Jun. 2008.

Fengbing Li He received his B.S. degree in 2008 from the School of Electrical Engineering, Chongqing University, Chongqing, China, where he is currently pursuing the Ph.D. degree in electrical engineering after coming back from the mountains to support minority education. His research interests include energy storage system and microgrids.

Kaigui Xie He received the Ph.D. degree from the School of Electrical Engineering, Chongqing University, Chongqing, China, in 2001. He is currently a Professor with the School of Electrical Engineering, Chongqing University, Chongqing, China. His research interests include power system planning and reliability, analysis, electricity market, distributed generation and microgrids.

Bo Zhao He received the Ph.D. degree from the Department of Electrical Engineering, Zhejiang University, Hangzhou, China, in 2005. He is currently an Engineer with the Research Center, Electric Power Research Institute of State Grid Zhejiang Electric Power Corporation, Zhejiang, China. His research interests include distributed generation and microgrids.

Dan Zhou He received the Ph.D. degree from the Department of Electrical Engineering, Zhejiang University, Hangzhou, China, in 2011. He is currently an Engineer with the Research Center, Electric Power Research Institute of State Grid Zhejiang Electric Power Corporation, Zhejiang, China. His research interests include power electronics and microgrids.

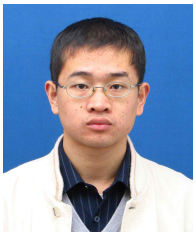

Xuesong Zhang He received the Ph.D. degree from the Department of Electrical Engineering, Zhejiang University, Hangzhou, China, in 2006. He is currently an Engineer with the Research Center, Electric Power Research Institute of State Grid Zhejiang Electric Power Corporation, Zhejiang, China. His research interests include relay protection and microgrids.

Jiangping Yang She received the M.S. degree from the School of Electrical Engineering, Chongqing University, Chongqing, China, in 2012. She is currently an engineer with the Ministry of Construction, State Grid Sichuan Electric Power Corporation Meishan Power Supply Company, Sichuan, China. Her research interests include smart distribution grid and microgrids.